A Translating Fluxmeter for the Determination of Boundary Data and the BEM-Based Magnetic Field Reconstruction

Melvin Liebsch[1], Stephan Russenschuck[1], Jens Kaeske[1,2], Anthony Beaumont[3], Pawel Kosek[3], Stefan Kurz[4]
[1]European Organization for Nuclear Research (CERN), Geneva, Switzerland
[2]Karlsruhe Institute of Technology (KIT), Germany
[3]Helmholtzzentrum fur Schwerionenforschung (GSI), Darmstadt Germany
[4]Federal Institute of Technology Zurich (ETH), Switzerland

Email: melvin.liebsch@cern.ch

***Abstract*—For the accurate tracking of charged-particle beams in accelerator magnets and spectrometers, a precise description of the magnetic flux density is required. For this reason, field maps based on magnetic measurement data are used to assess manufacturing errors and tolerances. Established measurement techniques are based on Hall sensors and the sampling of the magnetic flux density vector on a three-dimensional grid. While providing a high spatial resolution, accurate Hall sensor measurements require an elaborate calibration procedure and high-level maintenance. Moreover, the overall measurement duration to achieve a reasonable spatial resolution is significant. In this work, we present a new approach for the determination of three-dimensional field maps based on a so-called translating fluxmeter and a numerical post-processing technique employing a boundary element method (BEM). This approach is considerably more accurate, faster, and requires less maintenance than Hall sensor-based alternatives.**

I. Introduction

Boundary integral methods have been proposed for the field representation in beam-transport systems in [1]. Approaches for the accurate determination of boundary data from magnetic field measurements have been presented in [2] for integral fields, and in [3] for the post-processing of Hall probe measurement data. These methods are significantly faster than direct sampling on 2D and 3D grids, and more precise due to the smoothing property of the boundary integral equation.
However, Hall probe measurements are affected by systematic error sources due to temperature effects, sensor displacements, vibrations, and planar Hall effects [4]. The calibration and maintenance of these devices are, therefore, elaborate.
Induction coil measurements, on the other hand, provide a linear sensor response and do not require a complicated calibration procedure. Recent advances employ graded coils built with printed circuit board (PCB) technology to overcome the drawback of large active areas [5].
Building upon the previously mentioned advances, we have developed a new sensor system that enables the measurement of normal fluxes on the boundary surface of a box-shaped domain of interest, for instance, in spectrometer magnets. Based on the normal flux measurements, three post-processing steps are needed for the field reconstruction:

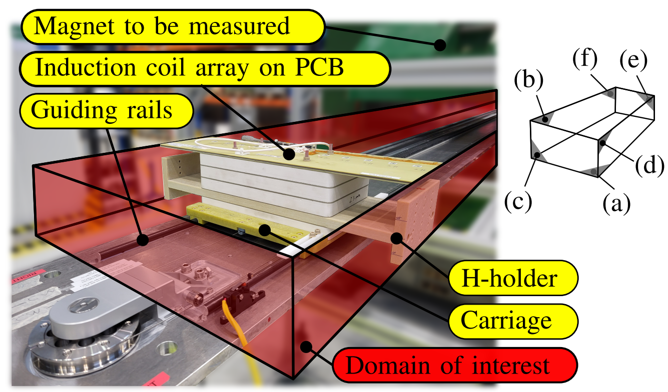

Figure 1. The translating fluxmeter is equipped with an H-shaped coil holder and vertical spacers. The system is set up to measure along the top (b) of the box-shaped domain of interest (top right).

(1) A deconvolution is needed in order to obtain the normal flux-density distribution on the boundary, and thus the Neumann trace.
(2) A Neumann-to-Dirichlet map to compute the missing Cauchy data.
(3) The field reconstruction by evaluating the boundary integral equation.

II. The Translating Fluxmeter

The translating fluxmeter is shown in Figure 1. It consists of a carriage mounted on rails and pulled by a stepper motor via stainless steel cords. A linear encoder with 5 μm resolution is used to measure the carriages' longitudinal position.
For the magnetic field measurement, the carriage can be equipped with an induction coil array. A special H-shaped coil holder was built to enable the measurement of normal fluxes along a box-shaped domain boundary (indicated as a red box in Figure 1). More details about the measurement system and signal processing can be found in [5].

III. The Neumann to Dirichlet Map

We consider a simply connected, open domain Ω in the vacuum region of the accelerator magnet. The magnetic scalar potential ϕ_{m}, defined by $\boldsymbol{H} = -\operatorname{grad}\phi_{\mathrm{m}}$ is harmonic in Ω, i.e., $\Delta\phi_{\mathrm{m}} = 0$.
The scalar potential ϕ_{m} can thus be computed from the Cauchy data (u and g) on the domain boundary $\partial\Omega$

$$\phi_{\mathrm{m}}(\boldsymbol{r}) = \int_{\partial\Omega} u(\boldsymbol{r}')\,\partial_{\boldsymbol{n}} G(\boldsymbol{r},\boldsymbol{r}')\,\mathrm{d}\boldsymbol{r}' - \int_{\partial\Omega} g(\boldsymbol{r}')\,G(\boldsymbol{r},\boldsymbol{r}')\,\mathrm{d}\boldsymbol{r}', \tag{1}$$

where $G(\boldsymbol{r},\boldsymbol{r}')$ is the Green's function of free space, $\partial_{\boldsymbol{n}}$ denotes the normal derivative, $u \in H^{1/2}(\partial\Omega)$ is the Dirichlet trace and $g \in H^{-1/2}(\partial\Omega)$ is the Neumann trace. While the Neumann trace can be determined from the normal component of the magnetic flux density $\mu_0 g = -\boldsymbol{n}\cdot\boldsymbol{B}$, the Dirichlet trace needs to be computed numerically.
Taking the Neumann trace, i.e., $\lim_{\boldsymbol{r}\to\partial\Omega}\partial_{\boldsymbol{n}}$ of the representation formula yields the so-called Neumann-to-Dirichlet map

$$(D\,u)(\boldsymbol{r}') = ((1/2\,I - K')g)(\boldsymbol{r}'), \tag{2}$$

which holds almost everywhere on $\partial\Omega$. See [6], for the definitions of the hypersingular, the adjoint double layer, and the identity operators D, K' and I, respectively.
For the numerical solution of the Neumann-to-Dirichlet map, we approximate the Cauchy data in the finite-dimensional function spaces $\mathcal{X}_u \subset H^{1/2}(\partial\Omega)$, and $\mathcal{X}_g \subset H^{-1/2}(\partial\Omega)$. Denoting by $\boldsymbol{u} \in \mathbb{R}^N$ and $\boldsymbol{g} \in \mathbb{R}^M$ the coefficient vectors for these approximations, we derive the discrete version of (2)

$$(\boldsymbol{D} + \boldsymbol{S})\,\boldsymbol{u} = (\boldsymbol{M} - \boldsymbol{K}^T)\,\boldsymbol{g}, \tag{3}$$

with the matrices $\boldsymbol{D} \in \mathbb{R}^{N\times N}$, $\boldsymbol{M} \in \mathbb{R}^{N\times M}$ and $\boldsymbol{K}^T \in \mathbb{R}^{N\times M}$. The stability matrix $\boldsymbol{S} \in \mathbb{R}^{N\times N}$ is imposing a gauge condition.
It remains to determine the coefficient vector $\boldsymbol{g}$ from the measurements of the translating fluxmeter.

IV. Deconvolution

The determination of the Neumann trace (i.e., the normal flux density), based on the flux measurements, is a two-dimensional deconvolution problem. In the following, we consider that the fluxmeter has performed measurements along the bottom side (a) of the box (see Figure 1), and we denote the k-th measurement by $\Phi_k^{(a)}$.
We express the Neumann trace on side (a) as a linear combination of L tensor product basis splines $\psi_l^{(a)}$, i.e., $g^{(a)} = \sum_{l=0}^{L} g_l^{(a)}\psi_l^{(a)}$. By collecting K measurements, we assemble the linear equation system

$$\boldsymbol{y}^{(a)} = \boldsymbol{X}^{(a)}\boldsymbol{g}^{(a)} \tag{4}$$

where $\boldsymbol{y}^{(a)} = \left(\Phi_1^{(a)}, ..., \Phi_K^{(a)}\right)^T$ is the vector of fluxes and $\boldsymbol{X}^{(a)} \in \mathbb{R}^{K\times L}$ is the design matrix with the elements

$$[\boldsymbol{X}^{(a)}]_{k,l} = -\mu_0 \int_{\mathcal{A}} s(\boldsymbol{r}_k + \boldsymbol{r}')\psi_l^{(a)}(\boldsymbol{r}_k + \boldsymbol{r}')\,\mathrm{d}\boldsymbol{r}'. \tag{5}$$

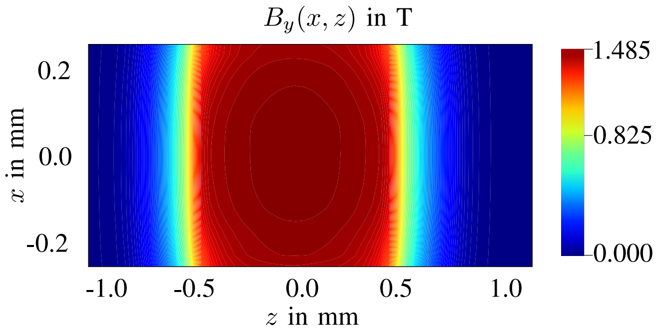

Figure 2. Normal flux density component on the bottom of the domain of interest (side (b)). The B_y component is derived from flux measurements in a normal conducting dipole magnet by deconvolution.

The function s is a geometry-dependent sensitivity function (see [5]), and $\mathcal{A}$ is the coil area. Accounting with the noise covariance matrix $\boldsymbol{R}$ for Gaussian random noise in the acquisition chain, we obtain $\boldsymbol{y}^{(a)} \sim \mathcal{N}(\overline{\boldsymbol{y}}^{(a)}, \boldsymbol{R}^{(a)})$ and $\boldsymbol{g}^{(a)} \sim \mathcal{N}(\overline{\boldsymbol{g}}^{(a)}, \boldsymbol{\Sigma}_g^{(a)})$ with the statistical moments

$$\left(\boldsymbol{X}^{(a)T}\boldsymbol{R}^{(a)-1}\boldsymbol{X}^{(a)}\right)\overline{\boldsymbol{g}}^{(a)} = \boldsymbol{X}^{(a)T}\boldsymbol{R}^{(a)-1}\overline{\boldsymbol{y}}^{(a)}, \tag{6}$$

$$\boldsymbol{\Sigma}_g = \left(\boldsymbol{X}^{(a)T}\boldsymbol{R}^{(a)-1}\boldsymbol{X}^{(a)}\right)^{-1}. \tag{7}$$

While the same approach is applied to the sides (b), (d) and (f), we set $g^{(c)} = g^{(e)} = 0$, for the open sides (c) and (e) where no measurements are taken, as the field has decayed sufficiently. Approximation errors in the deconvolution process can be controlled by a residual-based, adaptive knot-vector refinement.

V. Results and Conclusions

In Figure 2, we show the deconvoluted normal flux density on the bottom side (b) for a measurement in a normal conducting dipole magnet. Having determined the normal fluxes on all sides of the domain boundary, it is possible to reconstruct the interior potential and field by evaluating (1) or its derivative. In this way, the quantities of interest, i.e., field maps, derivatives, and harmonic expansions along a particle trajectory, can be computed with high accuracy, leveraging on the smoothing property of the boundary integral equation.

References

[1] A. Dragt, T. Stasevich, and P. Walstrom, "Computation of charged-particle transfer maps for general fields and geometries using electromagnetic boundary-value data," pp. 1776 – 1777 vol.3, 02 2001.

[2] M. Liebsch, S. Russenschuck, and S. Kurz, "Boundary-Element Methods for Field Reconstruction in Accelerator Magnets," *IEEE Trans. Magn.*, vol. 56, p. 7511104. 4 p, 2020.

[3] M. Liebsch, S. Russenschuck, and S. Kurz, "BEM-Based Magnetic Field Reconstruction by Ensemble Kálmán Filtering," *Computational Methods in Applied Mathematics*, vol. 23, no. 2, pp. 405–424, 2023.

[4] M. Liebsch, *Inference of Boundary Data from Magnetic Measurements of Accelerator Magnets.* PhD thesis, Technische Universität, Darmstadt, 2022.

[5] M. Liebsch, S. Russenschuck, and J. Kaeske, "An induction-coil magnetometer for mid-plane measurements in spectrometer magnets," *Sensors and Actuators A: Physical*, vol. 355, p. 114334, 2023.

[6] S. Rjasanow and O. Steinbach, *The Fast Solution of Boundary Integral Equations*. Berlin Heidelberg: Springer Science & Business Media, 2007.